Throughput and energy-aware routing for 802.11 based Mesh Networks

Antonio de la Oliva[a,*], Albert Banchs[a,b], Pablo Serrano[a]

[a]*Universidad Carlos III de Madrid, Avda. Universidad 30, 28911 Leganes (SPAIN)*
[b]*Fundacion IMDEA Networks, Avda. del Mar Mediterraneo, 28912 Leganes (SPAIN)*

Abstract

In this paper we propose a novel routing algorithm for 802.11 based wireless mesh networks called *Energy and Throughput-aware Routing* (ETR). The design objectives of ETR are i) to provide flows with throughput guarantees, and ii) to minimize the overall energy consumption in the mesh network. **To achieve these objectives, we first analyze the throughput performance of the mesh network. Based on this analysis, we target obtaining the set of feasible allocations in the wireless network, i.e., the *capacity region*, which results in a set of complex non-linear equations that are not adequate for optimization algorithms. To overcome this computational complexity we derive a set of linear constraints (referred to as *linearized capacity regions*) which provides a much simpler formulation at a slightly reduced accuracy.** By feeding these linear constraints into an *integer programming* formulation, we then propose a routing algorithm that admits as many flows as possible while satisfying their throughput guarantees. This algorithm is further extended to account for energy considerations by devising a routing algorithm that uses as few nodes as possible, which allows switching off the unused nodes and thus save energy. The proposed approach is thoroughly evaluated and shown to outperform previous approaches very substantially both in terms of throughput and energy consumption.

Keywords: 802.11, Capacity Region, Energy Efficiency

*Corresponding author
 Email addresses: `aoliva@it.uc3m.es` (Antonio de la Oliva), `banchs@it.uc3m.es` (Albert Banchs), `pablo@it.uc3m.es` (Pablo Serrano)

1. Introduction

In the last few years, mesh networking has emerged as a cost effective and efficient solution for realizing backhaul networks to provide mobile users with potentially high quality services. The multihop wireless network architecture of mesh networks enables them to efficiently cover large areas without requiring many interconnections into a wired infrastructure. Furthermore, mesh networks are dynamically self-organized and self-configured, which ultimately results in reduced up-front cost and lower network maintenance costs for the operator. Along these lines, many major operators have already considered wireless mesh networks (WMNs) as a technology for their wireless Cities initiatives [1][1].

A critical concern for operators is to provide their users with service guarantees, which imposes some constraints on the performance of the mesh backhaul. Providing service guarantees to mobile devices, while preserving flexibility and cost efficiency, is a great challenge not supported by current technology, due to wireless mesh inherent limitations.

Another chief concern for operators is energy consumption. Indeed, nowadays it is a widespread goal to reduce the energy consumed by telecommunication networks, with initiatives such as *Green Touch*[2] that aim at reducing the energy consumption in networks by a factor of 1000. In addition to environmental reasons, the electricity bill is a major driver that pushes operators towards energy savings. Along these lines, it is highly desirable to minimize the energy consumed by operators' backhaul networks and in particular mesh-based backhauls. Despite this, the development of energy efficient mesh networks has received relatively little attention to date.

Following the above, we propose a novel routing solution for 802.11 based-WMNs to provide flows with throughput guarantees while optimizing the energy consumption. The proposed routing algorithm targets a network owned by an operator and relies on a centralized entity implementing resource allocation and admission control mechanisms. It builds on a linearized model of the capacity region of IEEE 802.11 DCF, which provides an accurate model of the set of feasible allocations at a low computational flexibility, thus supporting the execution of optimization algorithms in a timely manner.

[2]http://www.greentouch.org/

The key contributions of this paper are:

- We propose a novel way to represent the capacity region of a set of stations sharing the wireless medium, which we refer to as *linearized capacity region*, and compute the corresponding parameters that define this region for the case of 802.11. The linearized capacity region is devised with the aim of aiding the design of optimal and efficient networking algorithms.

- Based on the information provided by the *linearized capacity region*, we design a novel optimal routing algorithm for wireless mesh networks that admits as many users as possible to the network while providing them with the desired throughput guarantees.

- We design an extension to our routing algorithm that, in addition to providing throughput guarantees, minimizes the total energy consumed by the mesh network. This is achieved by switching off as many mesh routers as possible.

After a thoroughly evaluation of the performance of the resulting approach, by means of simulations and numerical results, we show that the proposed algorithm can route at least twice as much throughput as **compared approaches (Shortest path, ETX and ETT)** and, for a given throughput demand, it can save up to 40% of energy.

The rest of the paper is structured as follows. In Section 2 we present the network model and assumptions upon which our work relies. Section 3 analyzes the throughput performance of a set of 802.11 stations sharing the wireless medium, it obtains the capacity region from this analysis and then linearizes this region. This *linearized capacity region* concept is validated by means of **simulations (throughput model) and comparison with the exact analytical model for different scenarios**. Section 4 proposes a routing algorithm that provides throughput guarantees (based on the *linearized capacity region*) and minimizes energy consumption. The performance of the proposed algorithm is evaluated, both in terms of throughput and energy, via simulation. Finally, Section 5 reviews some related work and Section 6 closes the paper with some final remarks.

2. Network model

In the following we present the network model upon which our work is based as well as the assumptions upon which we rely.
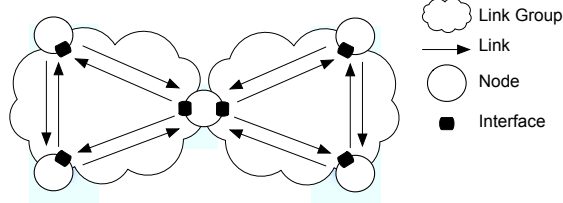
Figure 1: Link group concept.

Our network model is based on the notions of *link* and *link group*. We say that there is a *link* between two interfaces if these two interfaces operate on the same channel and can establish direct communication. We further define a *link group* as the set of interfaces ($n \geq 2$) that operate on the same channel and can directly communicate with each other[3]. In Fig. 1 we illustrate a WMN with 2 *link groups* consisting of 6 *links* each.

In this paper we focus on a scenario where the channels of the wireless mesh networks are carefully assigned in order to avoid undesired interferences. This is typical in planned networks such as e.g. an operator-owned network where channels are centrally assigned in a way that overall interference in the network is minimized (see e.g. [2]).

Following the above target scenario, a key assumption of our paper is that the channel assignment algorithm results in the following:

- All the interfaces that belong to the same *link group* are assigned to the same channel and are in the transmission (and collision) range of each other.

- The stations that do not belong to the same *link group* do not cause transmission errors to each other, either because they are assigned to different non-overlapping channels or because (although using an overlapping channels) they are physically located far enough from each other.

Following the above assumption, a transmission from an interface will be successful as long as it does not interfere with any transmission of the same *link group*, independently of whether the interfaces that belong to other link groups transmit or not. As a result, *with our model throughput performance can be ana-*

---

[3]Note that this concept only considers links that contend for channel access with each other.

lyzed independently at each link group. This is the basis of our throughput analysis of Section 3.

The above assumption is supported by our experimental work of [3]. In this work, we set up a network based on 802.11a and showed that as long as the separation between channels of different link groups is large enough, they do not interfere with each other. Following this, we deployed a mesh network [4] with careful channel assignment in order to meet the requirements stated above, and verified experimentally that these requirements are indeed satisfied.

In addition to channel assignment, link adaptation techniques support the use of modulation schemes that prevent external interference to cause any transmission error. While in this paper we do not focus on the design of such techniques, we consider that they are being used and take the modulation scheme used by each interface as input.

Finally, in terms of energy consumption, we use a simplified model that considers that devices consume a constant power when switched on while neglecting the energy dedicated to individual transmissions. This model follows the "on-off" energy profile introduced by Restrepo et al. in [5], which is based on the measurements by Corliano and Hufschmid in [6]. These measurements show that the energy consumed by the transmissions of some typical wireless devices accounts only for a very small portion of their overall consumption. **The "on-off" model is well known in the literature and has been adopted in other works such as [7] or [8].** Following this model, our objective in this paper is to switch off as many devices as possible in order to minimize the overall energy consumed by the wireless mesh network[4].

3. Throughput analysis

Following the *link group* concept presented above, the throughput of the wireless mesh network can be computed by considering each link group independently. In the following we study the throughput performance of a link group:

- We first compute all the feasible throughput combinations in the link group, i.e., the throughputs that each of the links in the link group can have. We

---

[4]**The proposed energy algorithm aims at maximizing the number of nodes that can be switched off while the network is operating under low load, e.g. night hours. In contrast, when the network operates under high loads, i.e., peak-hour traffic, all nodes are likely to be required to serve the incoming traffic (as network dimensioning is typically performed considering the traffic demand at peak hours).**

denote the set of all feasible combinations by *link group capacity region*.

- We then linearize the above capacity region, obtaining the *linearized capacity region*. The main features of this region are: i) it contains a subset of the feasible throughput combinations, and ii) it allows checking whether a given throughput combination is contained in the region or not by means of a simple *linear* equation. As we will see in the next section, these features are very useful when dealing with optimization problems.

The validation of this model is done by assessing the performance of the resulting *linearized capacity region* as compared against the *exact capacity region*. Results show that the linearized capacity region covers most of the exact region, which means that performance will not be significantly degraded by employing the linearized capacity region instead of the exact one.

3.1. Link group capacity region

Let us consider a link group with n nodes (i.e., each of these nodes has an interface that belongs to the link group). Let us denote by r_i the throughput that node i receives in this link group. In the following we analyze the set of possible throughput combinations $\{r_1, r_2, \ldots, r_n\}$ in the link group. We denote the set of possible combinations as *capacity region* and say that a given combination belongs to the *boundary of the capacity region* if we cannot increase the throughput allocated to any node without decreasing the throughput of some other node.

Let τ_i be the probability that the interface of node i that belongs to the link group transmits at a given slot time. For simplicity, in the following we refer to this event simply as a *transmission of node i*. This transmission will be successful if and only if no other node of the link group transmits simultaneously. Thus,

$$p_{s_i} = \tau_i \prod_{j \in L \setminus i} (1 - \tau_j) \tag{1}$$

where L is the set of nodes of the link group.

Similarly, the probability that a slot time is empty or contains a collision are computed according to

$$p_e = \prod_{j \in L} (1 - \tau_j) \tag{2}$$

$$p_c = 1 - p_e - \sum_i p_{s_i} \tag{3}$$

Following the above, the throughput of a node i in the link group can be computed as

$$r_i = \frac{p_{s_i} l}{\sum_i p_{s_i} T_{s,i} + p_c T_c + p_e T_e} \tag{4}$$

where l is the length of a packet and $T_{s,i}$, T_e and T_c are the average durations of a successful transmission of node i, an empty slot time and a collision, respectively.

In order to compute r_i, we need to obtain the τ_i's. For this, we distinguish between saturated and non-saturated nodes. Saturated nodes are those whose sending rate is larger than their throughput, and hence always have a packet ready for transmission. According to [9], the transmission probability of these nodes satisfies the following condition:

$$\tau_i = \frac{2}{1 + W + p_{c,i} W \sum_{j=0}^{m-1} (2p_{c,i})^j} \tag{5}$$

where W and m are the CW_{min} and maximum backoff stage parameters, which are given by the 802.11 standard [10], and $p_{c,i}$ is the conditional collision probability of the node, which is computed according to

$$p_{c,i} = 1 - \prod_{j \in L \setminus i} (1 - \tau_j) \tag{6}$$

For the case of non-saturated nodes, throughput is equal to the sending rate S_i, and therefore we can isolate their τ_i from Eq. (4), which yields

$$\tau_i = \frac{S_i (\sum_i p_{s_i} T_{s,i} + p_c T_c + p_e T_e)}{l \prod_{j \in L \setminus i} (1 - \tau_j)} \tag{7}$$

With the above model, given the input rates of the nodes of a *link group*, we can compute the corresponding τ_i's, depending on whether they are saturated or not, and the corresponding throughputs $\{r_1, \ldots, r_n\}$. This terminates our throughput model. Based on the above throughput model of a link group, in the following we obtain the capacity region of the link group.

Our computation of the capacity region is based on the observation that, in the boundary of the capacity region, one or more stations are saturated, as otherwise there is at least one station that can increase its throughput without decreasing the throughput of the other stations. Based on this observation, we compute the boundary of the capacity region as follows:

- We divide all the nodes in the link group into two sets, the set of saturated nodes and the set of non-saturated nodes, and consider all possible sets of saturated stations.

- The τ_i of the saturated nodes is given by Eq. (5). Since all non-saturated nodes will surely have a smaller τ_i, we sweep across the τ_i of the other nodes in the range $(0, \tau_{sat})$, where τ_{sat} is the τ_i of the saturated nodes[5].

Each of the steps of the above iteration provides a boundary to the capacity region, and any point inside this boundary belongs to the capacity region. This terminates the analysis of the exact capacity region. The performance of this analysis is validated against simulations in Section 3.3.1.

3.2. Linearized capacity region

Obtaining the capacity region as described above is complex, as it requires solving a non-linear system of equations on the τ's. This way, determining wether a given throughput allocation $\{r_1^*, \ldots, r_n^*\}$ is feasible in a certain link group is computationally expensive. Therefore, the above analysis cannot be used to solve optimization problems that need a simple way to determine whether a given allocation is feasible or not.

In order to overcome this limitation, we propose the following linear equation to model the capacity region of the link group,

$$\sum_{i \in L} w_i r_i < C \qquad (8)$$

where w_i is the weight of node i and C is the capacity of the link group. **As will be shown later on this section, the weights determine the set of throughputs allowed by the linearized capacity region. The computation of the weight values to optimize the linearize capacity is one of the key contributions of this paper**. This *linearized capacity region* allows determining whether a given allocation $\{r_1, \ldots, r_n\}$ is feasible or not by computing a simple *linear equation*. As we will see in the next section, this feature enables the use of efficient optimization techniques such as *linear programming* or *integer programming*.

---

[5]**The computation of the τ for all nodes is a complex operation that requires solving a multi-variable non-linear equations system. In order to solve this, a numeric method must be applied, which in our case is based on the trust-region dogleg method [11].**

The rest of this section is devoted to the computation of the parameters that define the linear capacity region (i.e., w_i and C). While computing these parameters, we aim at the following objectives:

- The linearized capacity region must be entirely contained within the exact capacity region. This guarantees that any throughput allocation inside the linearized capacity region is actually feasible.

- The linearized capacity region should cover the exact capacity region as much as possible. The reason is that we would like to avoid that a given desired allocation $\{r_1, \ldots, r_n\}$ that is feasible according to the exact capacity region is not contained inside the linearized capacity region.

Fig. 2 illustrates that there are several degrees of freedom when computing the capacity region, as we can choose different slopes for the each dimension (the figure shows three different options: a, b and c). In this paper, in order to cover the exact capacity region as much as possible, we choose the slopes of the capacity region such that, when crossing each axis, the values of the exact and linearized capacity regions are proportional (this corresponds to the option b in Fig. 2):

$$\frac{w_i}{w_j} = \frac{R_j}{R_i} \tag{9}$$

where R_i is the throughput of node i when crossing axis i (i.e., when the throughput of all nodes but i are zero).

Without loss of generality, we take $w_1 = 1$, which allows us to compute the values of the remaining weights w_i following Eq. (9). The pending challenge is the computation of the link group capacity C; to find it, we look for the point where the following function takes a minimum

$$\sum_{i \in L} w_i r_i \tag{10}$$

where the r_i's are the throughput values in the boundary of the exact capacity region[6].

---

[6]**Note that a given throughput combination belongs to the boundary of the capacity region if we cannot increase the throughput allocated to any node without decreasing the throughput of some other node.**
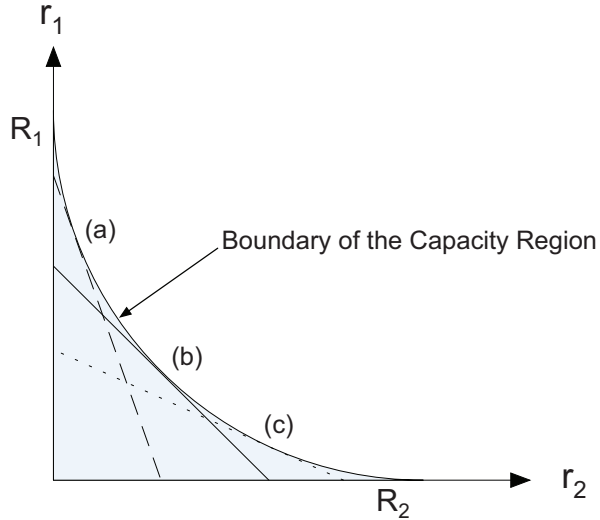
Figure 2: Linearized capacity region.

Note that, with the above, the boundaries of the exact capacity region satisfy

$$\sum_{i \in L} w_i r_i > C \tag{11}$$

and hence any point inside the linearized capacity region is guaranteed to be contained in the exact capacity region.

To find the minimum of the function of Eq. (10), we perform a search over all the τ_i's with the following constraint. Since we are at the boundary of the capacity region, the node with the highest throughput will be saturated, and hence its τ_i has to satisfy Eq. (5). Without loss of generality, we denote the node with the highest throughput as node 1.

To find the minimum of the function $\sum_i w_i r_i$ with the above constraint on τ_1, we apply the Lagrange multiplier as follows:

$$L(\tau_i, \lambda) = \sum_{i \in L} w_i r_i - \lambda \left(\tau_1 - \tau_1(p_{c,1}) \right) \tag{12}$$

where $\tau_1(p_{c,1})$ is the expression of τ_1 as a function of $p_{c,1}$ as given by Eq. (5).

Taking the partial derivatives and forcing that they are zero, we obtain

$$\frac{\partial L}{\partial \tau_j} = \frac{\partial \sum_i w_i r_i}{\partial \tau_j} + \lambda \frac{\partial \tau_1(p_{c,1})}{\partial \tau_j} = 0 \tag{13}$$

10

Given that the τ_i's are very small, the partial derivative on $\tau_1(p_{c,1})$ can be neglected

$$\frac{\partial \tau_1(p_{c,1})}{\partial \tau_j} \approx \frac{1}{W} \approx 0 \tag{14}$$

which yields

$$\frac{\partial L}{\partial \tau_j} = \frac{\partial \sum_i w_i r_i}{\partial \tau_j} = 0 \tag{15}$$

If we neglect the time wasted on idle slots when only one station is transmitting, the throughputs R_i are approximately inversely proportional to the durations of successful transmissions $T_{s,i}$. Combining this with Eqs. (4) and (9) leads to

$$\sum_i w_i r_i = \frac{1}{T_{s,1}} \frac{\sum_i p_{s_i} T_{s,i}}{\sum_i p_{s_i} T_{s,i} + p_c T_c + p_e T_e} \tag{16}$$

If we take the partial derivative of the above equation and neglect all the terms on τ_i of order 2 or above in the numerator (which gives a good approximation considering that $\tau_i \ll 1$), we obtain

$$\frac{\partial \sum_i w_i r_i}{\partial \tau_j} = \frac{T_e}{T_{s,1}} \frac{T_{s,j} + 2T_{s,j}\tau_j - 2\sum_k T_{s,j}\tau_k}{(\sum_i p_{s_i} T_{s,i} + p_c T_c + p_e T_e)^2} = 0 \tag{17}$$

From operating in the above equation,

$$\tau_j = \sum_k \tau_k - \frac{1}{2} \tag{18}$$

which yields

$$\tau_j = \tau_k \ \forall j, k \tag{19}$$

We conclude that the function $\sum_i w_i r_i$ takes a local maximum or minimum when all τ_i's take the same value. Based on this, we proceed as follows to compute the link group capacity C. First, we compute the value of the function $\sum_i w_i r_i$ when all nodes are saturated (note that they have the same τ_i in this case). We denote the value that the function takes at this point by R.

Since R could be a local maximum or minimum (see Fig. 3), the minimum of the function could be located at one of the extremes of the region considered, in particular at one of the axes. Note that at a given axis j, node j will be allocated
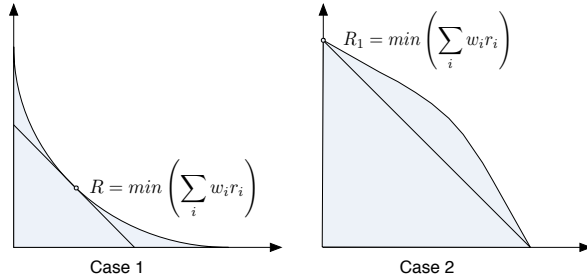
11

Figure 3: Local maximum and minimum.

a throughput R_j and the other nodes will be allocated no throughput. Then, with our setting of the w_i's,

$$\sum_i w_i r_i = w_j R_j = \frac{R_1}{R_j} R_j = R_1 \qquad (20)$$

Therefore, the function $\sum_i w_i r_i$ takes the same value (R_1) at any edge. Note that R_1 is the throughput that node 1 receives when the other nodes of the link group do no transmit, and can be easily computed following the previous throughput analysis.

Based on the above, we compute C as the minimum between R_1 and R:

$$C = min(R_1, R) \qquad (21)$$

With the above, we have obtained the weights w_i and the link group capacity C, which terminates the computation of the *linearized capacity region*.

3.3. Performance evaluation

In this section we first validate the accuracy of the throughput model presented above, and then assess the efficiency of the linearized capacity model. **In order to evaluate the accuracy of the throughput model, we compare the analytical results obtained of applying the mathematical model explained in section 3.1 to simulation based results. On the other hand, the assessment of the efficiency of the linearized capacity model is performed completely analytically.**

The simulator tool **used for the model validation** is an event driven simulator based on OMNET++[7] that closely follows the details of the 802.11 protocol. In

---

[7]http://www.omnetpp.org/

Scenario					R_{sat} (Mbps)	
N_{sat}	N_{nonsat}	C_{sat}	C_{nonsat}	R_{nonsat}	Ana.	Sim.
1	1	11	11	0.5	6.48	6.49
		11	11	1.0	6.04	6.05
		11	11	2.0	5.15	5.16
		11	5.5	2.0	3.77	3.78
		11	1	0.5	2.98	3.01
		1	11	0.5	0.83	0.83
		1	1	0.25	0.65	0.66
2	2	11	11	0.5	6.36	6.36
		11	11	1.0	5.36	5.36
4	4	11	11	0.5	5.17	5.18

Table 1: Validation of the throughput model: Experiment I

our simulations, we assume the use of the **802.11b/g** physical layer and 1500 bytes frames.

3.3.1. Model validation

We performed several experiments in order to validate the throughput model presented above. To this aim, we considered different heterogeneous scenarios and compared the results obtained from simulation against those computed using the analytical model. **Two experiments were performed, which results are presented in Table 1 and 2. The first experiment corresponds to different scenarios were several stations share the same channel, with different throughput requirements.** To generate the different scenarios, we varied the number of saturated and non-saturated nodes (denoted with N_{sat} and N_{nonsat}, respectively), the corresponding modulation rates (C_{sat} and C_{nonsat}), and the input rate generated by the non-saturated stations (R_{sat}). We assessed the accuracy of the model by computing the throughput obtained by the saturated stations (R_{sat}) using the model (Ana.) and using simulations (Sim.). The results are presented in Table 1, where each simulation value corresponds to the average of 10 simulation runs[8].

The second experiment corresponds to the same scenario used in section 3.3.3 to validate the linearized capacity region. In this experiment (more detailed in section 3.3.3) a set of n nodes share a link group. Each node sends

---

[8]Note that for each scenario the 95%-confidence interval, not shown in the Table, was smaller than 1% of the average value.

Scenario	N	Simulation (Mbps)	Analytical (Mbps)
Single Rate (11Mbps), $\alpha = 0.5$	8	6.80	6.83
	16	6.30	6.1
	32	5.10	5.2
Single Rate (11Mbps), $\alpha = 0.1$	8	6.92	6.93
	16	6.92	6.93
	32	6.92	6.93
Two Rates ($\frac{1}{2}$ stations $\{11, 5.5\text{Mbps}\}$), $\alpha = 0.5$	8	4.84	4.83
	16	4.22	4.25
	32	3.59	3.58
Multiple Rates ($\frac{1}{4}$ stations $\{11, 5.5, 2, 1\text{Mbps}\}$), $\alpha = 0.1$	8	6.52	6.53
	16	6.52	6.52
	32	6.52	6.52
Multiple Rates ($\frac{1}{4}$ stations $\{54, 36, 24, 18\text{Mbps}\}$), $\alpha = 0.1$	8	30.21	30.88
	16	30.21	30.87
	32	30.21	30.87
Multiple Rates ($\frac{1}{4}$ stations $\{54, 36, 24, 18\text{Mbps}\}$), $\alpha = 0.5$	8	15.98	15.99
	16	13.43	13.41
	32	10.67	10.68

Table 2: Validation of the throughput model: Experiment II

one flow to one of its neighbors forming a chain topology. The rate of each flow varies following the formula:

$$\frac{r_{i+1}}{r_i} = \frac{\alpha}{1-\alpha} \tag{22}$$

where α is a variable parameter that we use to set different throughput distributions ($\alpha = 0.5$ corresponds to equally distributing throughput among all flows, while smaller values of α yield to uneven distributions). The comparison between the analytical model results and the simulator are presented in Table 2.

The results of both experiments, show that the numerical values obtained follow very closely those resulting from the simulations. Indeed, for all the considered scenarios, the difference between the analytical and simulation results falls below 1%. We conclude from these results that the analytical model upon which our work is based is very accurate.

3.3.2. Linearized capacity region - Two Nodes

We next validate the accuracy of the linearized capacity region. To this aim, we numerically compute the set of feasible throughputs according to the exact capacity region computed in Section 3.1 and compare it against the set of feasible throughputs resulting from the linearized capacity region obtained in Section 3.2.

We first consider a scenario consisting of an 802.11b WLAN where two nodes share the same link group, and then compare the resulting capacity region for four different cases, depending on the modulation scheme that each node is using. In the first case both stations use a fixed modulation rate of 11 Mbps, which results in the capacity region depicted in Fig. 4, where the exact capacity region is plotted with a continuous line and the linearized one with a dashed line. We observe that the linearized capacity region covers most of the area of the exact capacity region, which confirms the efficiency of the proposed linearization.

Figs. 5, 6 and 7 show the exact capacity regions for the following modulation rates: $\{5.5Mbps, 11Mbps\}$, $\{1Mbps, 11Mbps\}$ and $\{1Mbps, 1Mbps\}$, respectively. We observe that, for all these cases, the linearized capacity region follows the exact one very closely, which confirms the efficiency of the proposed approach also for the case of heterogeneous modulation rates.

Finally, to complete the validation of the linearized capacity region for two stations, we computed the difference between the area covered by the exact capacity region and the area covered by the linearized capacity region (see color filled part on Fig. 8). This difference was computed for different
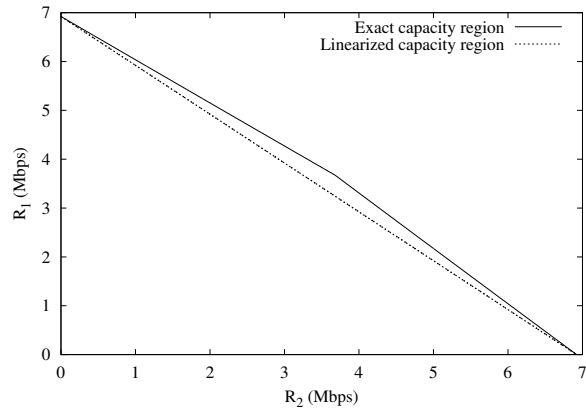
15

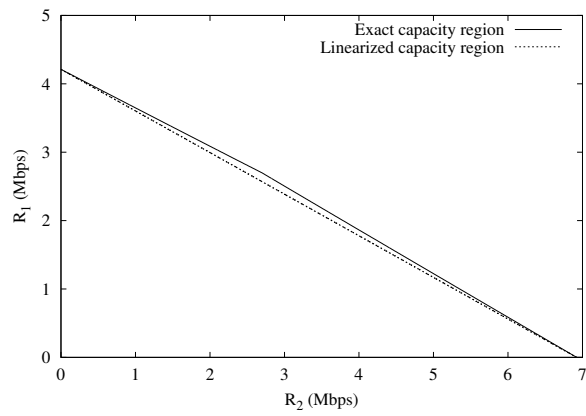Figure 4: Two nodes, homogeneous rates, 11 Mbps.

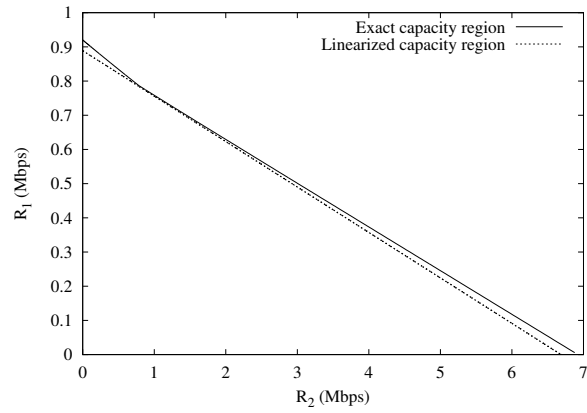Figure 5: Two nodes, heterogeneous rates, 5.5 and 11 Mbps.

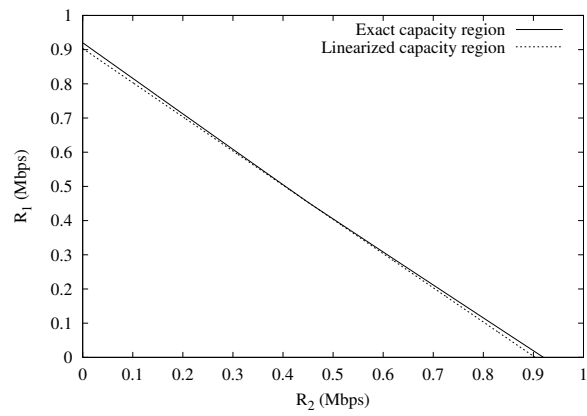Figure 6: Two nodes, heterogeneous rates, 1 and 11 Mbps.

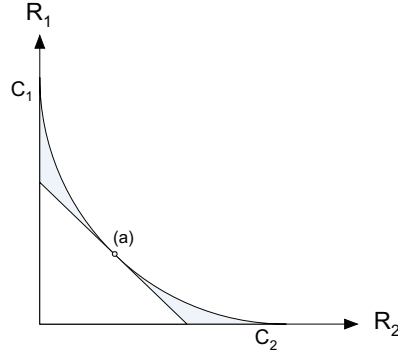Figure 7: Two nodes, homogeneous rates, 1 Mbps.

Figure 8: Difference between the areas covered by the capacity region and its linearization

IEEE 802.11b			IEEE 802.11g		
$R_1(Mbps)$	$R_2(Mbps)$	Difference (%)	$R_1(Mbps)$	$R_2(Mbps)$	Difference (%)
11	11	5.7	54	54	2.57
11	5.5	2.85	54	36	0.61
11	1	3.41	54	18	2.12
5.5	5.5	2.28	36	36	0.53
5.5	1	3.53	36	18	2.12
1	1	1.7	18	18	1.53

Table 3: Percentage of area not covered by the linearized capacity region

combinations of 802.11b and 802.11g transmission rates, the results are pre-sented in Table 3. The conclusions obtained from these results confirm the previous assumption, the area covered by both, the exact and the linearized capacity regions differs in a small percentage (always lower than a 6% in our results), even more, this difference decreases as higher rates are used.

3.3.3. Linearized capacity region - Multiple Nodes

All the above experiments validate our scheme for the case of a link group with two nodes. In order to assess the impact of larger link groups, we evaluated a scenario consisting of a link group with n nodes, where each node i sent a throughput r_i as follows:

$$\frac{r_{i+1}}{r_i} = \frac{\alpha}{1 - \alpha} \tag{23}$$

where α is a variable parameter that we use to set different throughput distribu-tions ($\alpha = 0.5$ corresponds to equally distributing throughput among all flows,
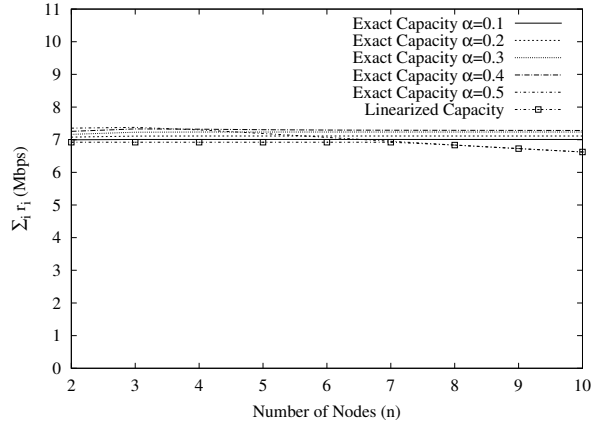
18

Figure 9: Multiple nodes, single rate.

while smaller values of α yield to uneven distributions).

Given this scenario, we considered three different cases based on the modulation rate used by nodes:

- The "single rate" scenario, where all nodes have a modulation rate of 11 Mbps.

- The "two rates" scenario, where half of the nodes transmit at a modulation rate of 11 Mbps and the other half at 5.5 Mbps.

- The "multiple rates" scenario, where one fourth of the nodes transmit at a modulation rate of 11 Mbps, 5.5 Mbps, 2 Mbps and 1 Mbps, respectively.

For each of these scenarios and a varying number of nodes n, we first compute the linearized capacity region. Then, for different values of the parameter α, we compared maximum of the sum of throughputs ($\sum r_i$) of all the feasible allocations as given by the exact capacity model against the one provided by the linearized capacity region. The resulting values for each of the three scenarios are depicted in Figs. 9, 10 and 11, respectively.

Note that in the single rate scenario the maximum achievable throughput as given by the linearized capacity does not depend on α, and therefore in Fig. 9 there is only one line drawn for the linearized capacity, which applies to all α values. On the other hand, for the cases with heterogeneous rates (Figs. 10 and 11) the maximum achievable throughput does depend on the value of the α parameter, decreasing as more throughput is given to those nodes with lower modulation rates.
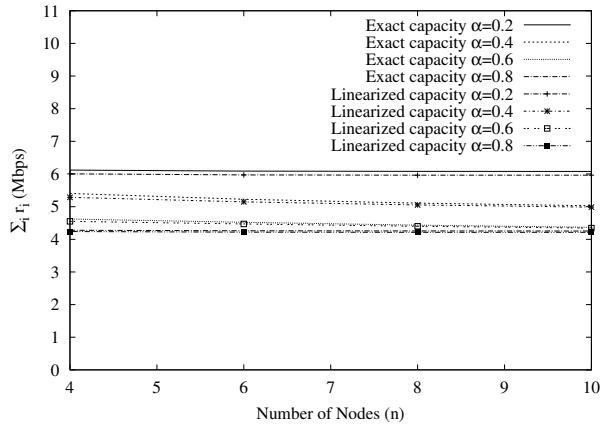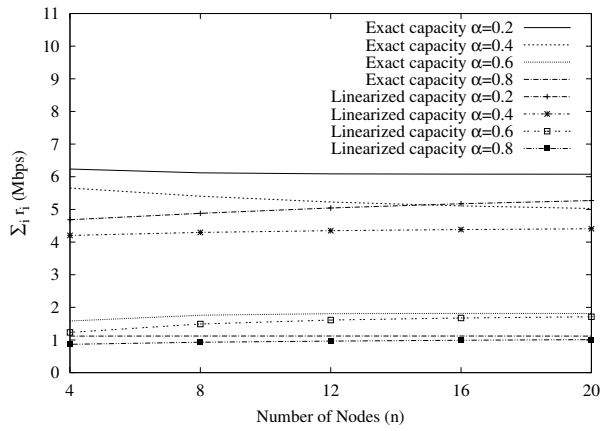
19

Figure 10: Multiple nodes, two rates.

Figure 11: Multiple nodes, four rates.

The main conclusion that we draw from the above results is that the number of nodes has a fairly small impact on the linearized capacity region. Indeed, for all scenarios the difference between the exact and the linearized capacity does not change noticeably with the number of flows. These results show that the conclusions given above for two nodes also hold for multiple nodes.

4. Routing algorithm

The key objective of the proposed linearized capacity region is to aid the design of efficient algorithms to optimize network performance. In particular, the proposed model allows to easily determine if a given throughput allocation is feasible, and therefore it supports the design of efficient optimization algorithms based on this ability.

In this section we present a routing algorithm for mesh networks called *Energy and Throughput-aware Routing* (ETR). The scheme relies on the proposed *linearized capacity region* to provide throughput guarantees. It is important to note that the routing algorithm is only an example to show the potential of the proposed concept. Indeed, the linearized capacity region can be used to solve other optimization problems such as, e.g., network planning or traffic engineering.

In the following we first present the basic routing algorithm which only takes into account throughput considerations, and then we extend the algorithm to account for energy consumption as well.

4.1. Basic Routing Algorithm

The basic version of our routing algorithm aims at admitting as many flows as possible while satisfying their throughput requirements. More specifically, given a scenario defined by:

- A mesh network consisting of a set link groups with the corresponding linearized capacity regions as computed in the previous section.

- A set of gateways, which provide connectivity to the Internet.

- A set of flow demands, each flow i originating at source node s_i and with a throughput requirement r_i.

We want to find a route for each flow to any of the gateways of the mesh network such that the throughput requirements of all flows are met and the number of admitted flows is maximized.

21

It can be easily seen that the above routing problem is *NP-hard*. Indeed, the problem can be viewed as a generalization of the well known *single-source disjoint paths* problem: this is a particular version of our routing problem in which all flows originate at the same source node, all link groups consist of two nodes and the flow requests are equal to the link group capacities. With this setting, our routing problem will try to find disjoint paths towards each gateway which is precisely what the *single-source disjoint paths* problem does. Since the *single-source disjoint paths problem* is known to be *NP-hard*, so is our problem. In the following, we present an integer programming (*IP*) formulation of our problem which we then solve by applying standard techniques.

The *IP* formulation of our problem is defined as follows. Let x_i be 1 if flow i is routed and 0 otherwise. Furthermore, let $y_{i,l}$ be 1 if the path chosen for flow i traverses link l and 0 otherwise, where (following the terminology introduced in Section 2) with *link* we refer to a pair of directly connected nodes. Given these variables, we want to find the allocation that satisfies

$$\max \sum_i x_i \tag{24}$$

subject to

$$x_i = \sum_{l \in s_i} y_{i,l}, \ \forall i \tag{25}$$

$$\sum_{l \in N_{in}} y_{i,l} = \sum_{l \in N_{out}} y_{i,l}, \ \forall N \tag{26}$$

$$\sum_{l \in L} w_l \sum_{i \in l} y_{i,l} r_i \leq C, \ \forall L \tag{27}$$

$$x_i \in \{0,1\}, \ \forall i \tag{28}$$

$$y_{i,l} \in \{0,1\}, \ \forall i,l \tag{29}$$

The above problem formulation aims at maximizing the number of routed flows ($\sum_i x_i$), subject to the following constraints.

- Eq. (25) imposes that in case flow i is routed, **there is one outgoing link from the source node of flow i** (s_i) for which $y_{i,l} = 1$, while the other $y_{i,l}$'s are zero.

- Eq. (26) imposes the flow conservation constraints, by guaranteeing that the sum of incoming flows to a node equals the sum of outgoing flows. We denote the set of incoming and outgoing links with N_{in} and N_{out}, respectively. Note that this equation applies to all nodes but sources and gateways.

- Eq. (27) imposes the capacity constraints for each link group L as given by our linearized capacity model. In particular, this equation imposes that the sum of the aggregated rates for each link, with the corresponding weight w_i, cannot exceed the link group capacity C.

- Finally, Eqs. (28) and (29) impose that flows cannot be split among different paths[9].

The above IP problem can be solved[10] by using standard relaxation techniques which first find a solution of the corresponding linear programming (LP) problem, in which the variables x_i and $y_{i,l}$ can take non-integer values, and then find an approximate solution to the IP problem by rounding these variables to integer values. **In particular, the technique that we have used in this paper is the one implemented on the GNU Linear Programming Kit (GLPK) and is based on a Branch and Bound method. More information of the actual algorithm implemented can be found in [14].**

By applying the above method, we obtain an approximation to the optimal routing strategy that provides throughput guarantees. Additionally, note that the proposed algorithm also implements the *admission control* functionality; indeed, when the algorithm does not find a route for all requests, this means they all cannot be accommodated and therefore a policy decision has to be made (e.g., the request that triggered the algorithm must be rejected).

4.2. Energy-aware Extension

In the following we extend the routing algorithm proposed in the previous section which, in addition to throughput considerations, aims at minimizing the energy consumption of the wireless mesh network. Following the discussion of Section 2, we minimize energy consumption by using as few nodes as possible to satisfy the throughput demands, while the remaining routers are switched off and thus do not consume energy. As a first step towards designing our energy-

---

[9]**Although there is some ongoing research work on techniques that allows splitting of the flows within the mesh network into different paths (such as the work being performed at the IETF Multipath TCP WG[12, 13]), these techniques have not yet been deployed in practical scenarios and a number of questions remain on their performance. Following this, we assume in this paper that flows are unsplittable, therefore the propped solution can be directly applied to current networks without extra functionality to support multipath.**

[10]**Given the problem is NP, herein with "solve" we refer to find an approximation to the solution.**
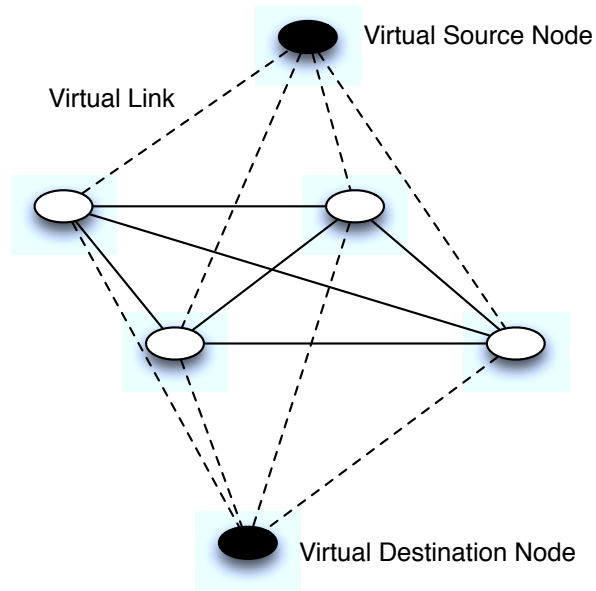
Figure 12: Virtual node algorithm representation

aware routing algorithm, we start by answering the following question: can the throughput demands of all the flows be satisfied while k of the routers are switched off? To answer this question, we formulate the following extension to the IP problem of the previous section, illustrated in Fig. 12:

- We introduce two virtual nodes in the network, namely, the Virtual Source node and the Virtual Destination node.

- We create one link between the Virtual Source node and each node in the mesh network, and another link between each node and the Virtual Destination node.

- The capacity of all virtual links is set equal to $n_{max}C_{max}$, where n_{max} is the maximum number of interfaces that a network node has, and C_{max} is the largest link group capacity.

- We introduce k virtual flows that are originated at one of the virtual nodes (the virtual source node) and terminate at the other (the virtual destination node).

- The throughput requirement of each virtual flow is set to $n_{max}C_{max}$.

- We introduce a new constraint on each node of the mesh, which is that the aggregated throughput that traverses a node cannot exceed $n_{max}C_{max}$.

With the above, we have that each of the nodes in the network can either route a virtual flow, which consumes its entire capacity and does not leave any resources for the normal flows, or route just normal flows. Therefore, the nodes that route virtual flows are not used for the normal flows and can be switched off. Note that the capacity of a node ($n_{max}C_{max}$) has been chosen such that a node that is not routing a virtual flow has enough capacity for all its normal flows.

Since we have a total of k virtual flows, if the problem can be solved and all flows can be routed, then we have found a routing solution that keeps k of the routers inactive, which answers the above question. In particular, the IP formulation of the new problem is as follows (where x_i, $y_{i,l}$ and r_i account both for the normal flows and links and the virtual ones):

$$\max \sum_i x_i \qquad (30)$$

subject to

$$x_i = \sum_{l \in s_i} y_{i,l}, \ \forall i \qquad (31)$$

$$\sum_{l \in N_{in}} y_{i,l} = \sum_{l \in N_{out}} y_{i,l}, \ \forall N \qquad (32)$$

$$\sum_{l \in L} w_l \sum_{i \in l} y_{i,l} r_i \le C, \ \forall L \qquad (33)$$

$$\sum_{l \in N_{in}} y_{i,l} r_i \le n_{max} C_{max}, \ \forall N \qquad (34)$$

$$x_i \in \{0, 1\}, \ \forall i \qquad (35)$$

$$y_{i,l} \in \{0, 1\}, \ \forall i, l \qquad (36)$$

With the above, we have answered the question whether the throughput demands can be satisfied with k of the nodes inactive. Based on this, we apply the following iterative algorithm in order to find the solution that leaves as many routers as possible switched off:

- We start with no inactive routers ($k = 0$) and see whether (by solving the above IP problem) the throughput demands can be satisfied.

- We next set $k = 1$ and solve the IP problem with this setting. If we can find a solution, this means that all flows can be routed while switching off one of the nodes.

- Then, we increase k by one unit and see whether the throughput demands can be satisfied with one additional node switched off.

- We proceed with the iteration on k until the demands can no longer be satisfied, which provides us with the maximum number of routers that can be switched off as well as the corresponding routing solution.

The above terminates the design of our *Energy and Throughput-aware Routing* (ETR) algorithm which minimizes the energy consumption in the network while satisfying the desired throughput guarantees. Note that the algorithm only requires as many executions of the IP problem solver as nodes can be switched off. Hence, as long as the original IP problem can be solved **within a timeframe of minutes** (which is the case with the technique we are using), the computational complexity of the proposed algorithm will be affordable **(as explained in section 4.1, the algorithm used is the Branch and Bound implementation of GLPK, an study of the complexity of this algorithm can be found in [15])**.

The performance of the ETR algorithm is evaluated in Section 4.4 in terms of throughput and energy, and it is compared against other routing algorithms for mesh networks.

4.3. Protocol Operation

The proposed ETR approach relies on two algorithms, one that computes the link group parameters, described in Section 3, and the routing algorithm itself, which has been explained above[11]. These algorithms are executed in two steps. In the following we describe the steps of our protocol operation, the network instances that execute each of the steps as well as the information conveyed between these different instances. This is illustrated in Fig. 13.

The first step of the protocol operation is the computation of the link group parameters. This computation is performed at each link group separately, by a

---

[11]**Note that the above algorithm is designed as an application example of the linearized capacity region model. As such, it is an off-line algorithm that requires the knowledge of all input flows to the network in order to optimize it. Nevertheless, the same concept and usage of the linearized capacity region can be applied to on-line algorithms such as the ones described in [16].**
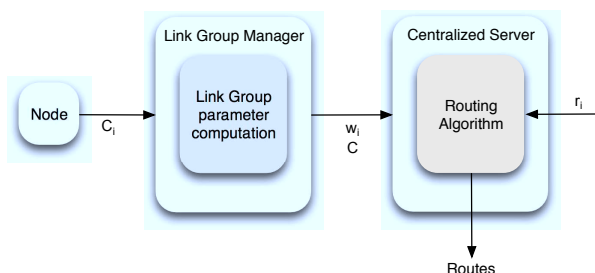
Figure 13: Protocol operation.

centralized entity in the link group which we denote by *link group manager*. The link group manager needs to retrieve the modulation scheme C_i used by the different nodes in the link group, and with this input it executes the algorithm of Section 3 in order to compute the parameters w_i and C of the link group.

The second step of the protocol operation is the execution of the routing algorithm itself. This algorithm is executed at a centralized location of the mesh network which we call the *Centralized Server*. This Centralized Server retrieves the parameters w_i and C of all the link groups in the mesh network. Also, it receives the requests of the different flows with the corresponding throughput guarantees. Based on these data, it executes the routing algorithm described above in order to decide whether the issued requests can be admitted or not and, in the affirmative case, the resulting routing. Once the routing decisions have been taken, the Centralized Server configures the computed routes in the network.

We argue that the above centralized architecture fits nicely the focus of this paper on an operator-owned network[12]. Indeed, network operators typically prefer to rely on centralized control to manage their networks. Additionally, the expected size of a mesh network will typically be limited[13], and hence centralized control does not raise any scalability issues.

---

[12]We note, however, that the proposed protocol does not necessarily need to be implemented by a centralized architecture and could also rely on a distributed routing protocol such as OSPF [17] which spreads the complete view of the network to all the nodes, which could then execute our ETR algorithm.

[13]**In the case of large mesh deployments (e.g. more than 100 nodes), the network can be partitioned in routing areas, and then the algorithm can be applied to each routing area independently. As long as these areas are composed of enough nodes and routes, the penalty incurred by partitioning will be low.**

4.4. Performance evaluation

In this section we assess the performance of the proposed ETR algorithm. We start by evaluating the throughput performance of the algorithm in terms of the amount of traffic that can be admitted into the network, as compared to traditional routing algorithms for mesh networks. Then we evaluate its energy performance in terms of the number of nodes that can be switched off without affecting network performance, under different traffic loads.

In order to conduct a performance evaluation independent of the chosen topology, we generated multiple random topologies and evaluated the average performance (and its deviation) among all topologies. To generate these random topologies we used the Hyacinth-Laca tool[14], which has been used in several well-known works such as [2] and [18]. This tool creates a mesh topology by randomly discarding nodes of a $N \times N$ grid of nodes until the desired size of the network is reached. In our experiments, we configured node count between 40 and 70 nodes (which yields a mean of 55 nodes) spread over an area of 400x400 square meters.

Once a topology is available, before performing a routing experiment we need to assign the channels used by each interface. For this purpose, we used a channel assignment policy that follows a Common Channel Set (CCS) configuration [19, 20, 21]. In order to calculate the modulation rate at which each node is able to communicate with its neighbors, we further used the curves of throughput versus distance given in [22].

The results shown on the next section are obtained using 128 simulation runs. For each run, we randomly select a topology from a set of 35 pre-computed random topologies. Each topology consists of a set of link groups, which are obtained by assigning the same channel to a set of nodes that are in a transmission range of each other. In average, each topology has 92 link groups, with values ranging between 52 and 164. Link groups are composed of 4 nodes in average, with a minimum size of 2 and a maximum size of 6. Given a topology, gateway and source nodes are randomly selected based on percentages specified by simulation scenario. All flows generate 100 kbps CBR[15] traffic. All sources start transmitting at the same time.

---

[14]Available at `http://www.ecsl.cs.sunysb.edu/multichannel/`

[15]For this work we have chosen CBR traffic although the model also works for other traffic processes as long as they are stationary [23].

4.4.1. Throughput performance

We evaluated routing performance for a varying number of gateways (10% and 25% of the nodes) and a varying density of source nodes (25% and 50% of the nodes). This yields to configurations with a minimum of 8 source nodes, a maximum of 31 and 16 in average, while for the case of gateway nodes their minimum is 4, their maximum is 17 and their average is 9. The metric used to evaluate routing performance is the maximum amount of traffic that can be admitted to the network while providing all flows with the requested throughput. As described above, for each experiment we provide the average amount of traffic that can be admitted into the network while satisfying all throughput requests, and its confidence intervals over a set of 128 simulations, with each simulation randomly selecting one of the 35 topologies.

The metric that we used to evaluate the routing performance is the maximum amount of traffic that can be admitted to the network while providing all flows with the same throughput[16]. For each experiment we generated a set of 35 random topologies, and we provide the average throughput performance and confidence intervals over the throughput resulting from **128 simulations (each simulation randomly selecting one of the 35 topologies).**

In order to show the performance improvement resulting from the proposed scheme (ETR), we compared it with well-known routing approaches for mesh networks, namely the Expected Transmission Count (ETX) [20], the Expected Transmission Time (ETT) [24] and Shortest Path (ShP). The results are given in Figs. 14 and 15 for the case of 10% and 25% gateway nodes, respectively.

From these results, we observe that independent of the density of gateways and sources, our proposal drastically outperforms the other approaches. In particular, while ETX, ETT and ShP provide performance numbers within the same order of magnitude, ETR admits more than twice the throughput than any of the other alternatives. This performance improvement of our proposal can be explained by the following two arguments:

- ETT and ETX are, like ShP, additive metrics, and as a result a path consisting of a few rather congested links may be preferred over a longer and less congested path, which harms throughput performance.

---

[16]**Note that the value of this metric corresponds to the point where the first flow demand that cannot admitted appears. Before reaching this point, all demands are admitted and served with the required throughput.**
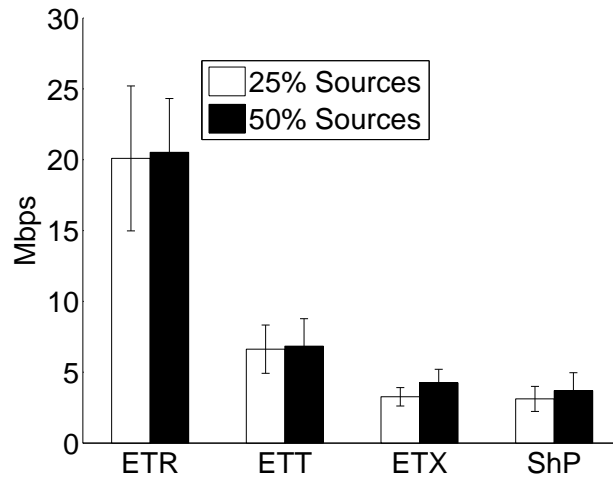
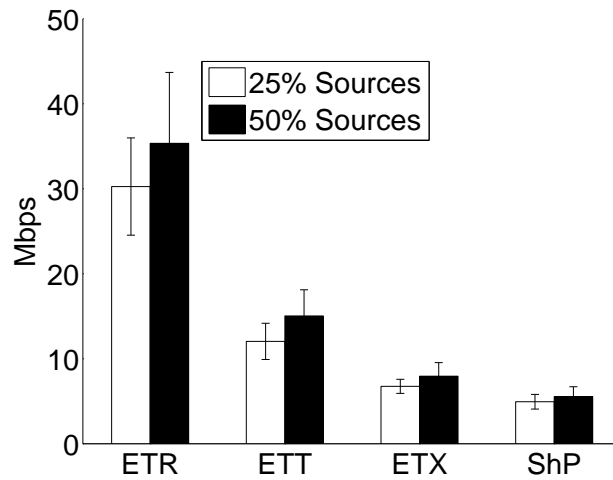Figure 14: Routing performance, 10% GW nodes.
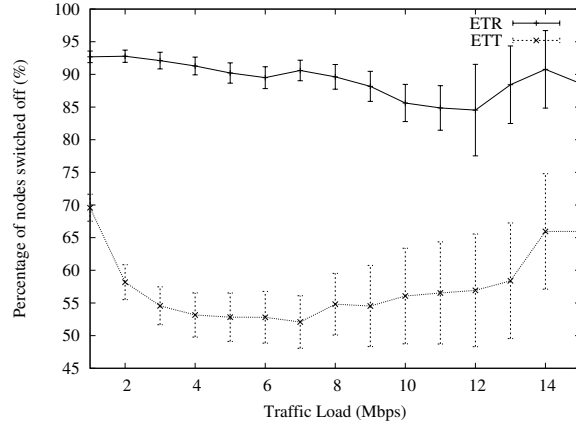

Figure 15: Routing performance, 25% GW nodes

Figure 16: Energy savings vs. ETT, 10 GW/Src nodes

- ETT and ETX do not take into account that the flows that belong to the same wireless link share the same resource; in contrast, our approach considers that allocating throughput to one flow harms the other ones in the same link.

We conclude from the above results that our method is effective in optimizing throughput performance, making an efficient use of the linearized capacity region and clearly outperforming previous approaches.

4.4.2. Energy performance

We next evaluate the performance of ETR in terms of energy consumption. To this aim, we use the same topology generation procedure as above **(see section 4.4)** and set the number of source nodes and gateway nodes equal to 10. We evaluate the performance of ETR by looking at the number of nodes that can be switched off and comparing it with the other routing strategies.

The comparison of our proposal against ETT, ETX and ShP is presented in Figs. 16, 17 and 18, respectively. In particular, these figures show the number of nodes that can be switched off with each of the strategies as a function of the load offered to the mesh network. It is important to note that in the graphs only consider load values that could be served by each of the routing strategies. The reason is that it would be unfair to compare ETR against another routing strategy when the load offered can only be served by ETR, since we would be comparing the two strategies under different loads.

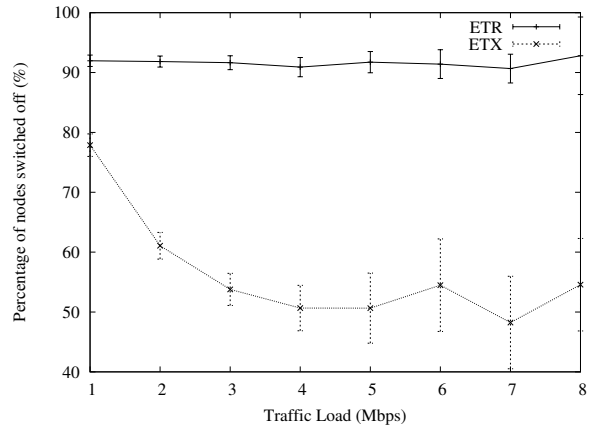The main results of the above figures can be summarized as follows:
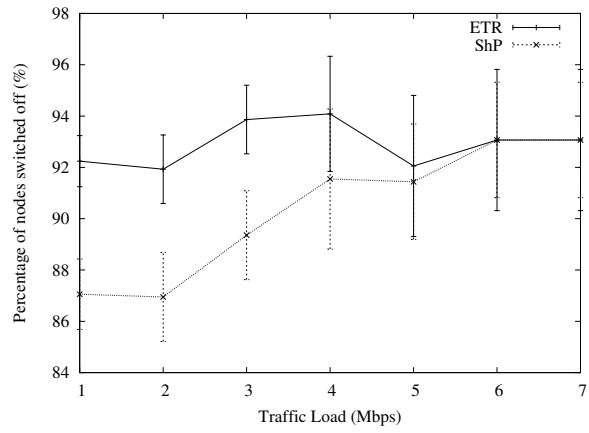
31

Figure 17: Energy savings vs. ETX, 10 GW/Src nodes

Figure 18: Energy savings vs. ShP, 10 GW/Src nodes

Description	Time (sec)
Time required to compute maximum number of nodes to shutdown	35
Time required to compute if a number k of nodes can be shutdown	24

Table 4: Times involved in computing ETR

- ETR outperforms the three routing strategies in terms of energy savings, as for all traffic loads it reduces the number of active nodes that are required to satisfy the given set of throughput demands.

- As compared against ETT and ETX, our proposal leads to substantial energy savings. Indeed, these two approaches use on average 40% of the nodes in the network to support the traffic load, while our approach only requires 10% of the nodes in order to provide the same service.

- On the other hand, compared against ShP our proposal does not result in very large improvements. The reason is that ShP routing uses a small number of nodes, which provides a good performance in terms of energy (and hence cannot be substantially improved by ETR) but (as we have seen in the previous section) provides very poor performance in terms of throughput.

From the above results, we conclude that ETR outperforms previous approaches very substantially: it outperforms ETT and ETX both in terms of throughput and energy, and although it does not outperform ShP very significantly in terms of energy, it drastically outperforms it in terms of throughput. These results therefore validate the performance of the proposed approach.

To end the validation of the ETR metric, Table 4 presents the averaged computational time[17] required for the different steps of the algorithm, for the topologies explained in section 4.4. As explained in section 4.2, the energy and routing optimization algorithm is computed in two steps. The first step corresponds to an iterative search algorithm, which iterates over the number k of nodes that can be shutdown. The second algorithm involved is the integer linear programming solver, that returns the routing and nodes that can be shutdown (and the feasibility of the solution).

The first row of Table 4, represent the average time required by the algorithm to find out the maximum number of nodes to shutdown for a given

---

[17]Computed in a standard desktop with a 3.06 GHz Intel Core 2 Duo processor.

33

topology and the lowest of the demands. This number is used as upper bound of the search algorithm. The second row corresponds to the average time required by each of the iterations of the algorithm, finding if for a certain demand, it is possible to shutdown k nodes. The search algorithm over k (number of nodes that can be switch off), takes a time to complete that is lineal with the second row of Table 4. It is important to note that this algorithm can be optimized by the use of well known numeric methods, such as golden search.

5. Related Work

In this work we propose a novel routing algorithm based on the computation of the linearized capacity region of an 802.11 WLAN. While computing the capacity region of a wireless network is an important research challenge in information theory, our contribution is to the best of our knowledge the first one to propose an efficient algorithm to compute the linear capacity region of the 802.11 DCF mechanism in order to support optimal routing and admission control. Indeed, the seminal work of Gupta et al. [25], as well as the extensions of [26, 27] to account for geometrical locations and transmission power, and the extensions of [28, 29] to account for infrastructure support, computed the upper bounds on the maximum capacity of the network and, as such, cannot be used to support a routing algorithm.

In the related literature, there are several works that jointly perform routing, scheduling and channel assignment in order to improve the performance of the network. In [30] the authors provide a fast mechanism to infer the feasibility of a certain end-to-end demand vector in a wireless mesh network, providing the joint routing and scheduling solution. They also provide two channel assignment algorithms, which allocate channels to links according to the traffic demand. In [31], authors evaluate the gain in performance resulting from a joint optimization of routing and scheduling in a multi-radio, multi-channel multi-hop network. Although both [30] and [31] are based on linear programming like our proposal, they do not consider contention, which represents a major difference with our work. In particular, reference [31] does not consider any MAC operation at all, while [30] assumes the presence of a mechanism that allows neglecting channel contention.

The impact of multihop, spatial reuse and power control on the capacity region is analyzed in [32] through the use of numerical techniques, by computing the set achievable rates for each possible configuration and then obtaining the convex hull

of the set of rate matrices. Although this work provides valuable insights on the impact of these parameters on the capacity region, it does not provide an efficient algorithm for its computation, which challenges its practical use.

In order to compute the linearized capacity region, we use the concept of Link Group. The idea behind the Link Group model is similar to the clique concept defined in graph theory. Given an undirected graph, a clique is defined as a subset of its vertices such that every two vertices in the subset are connected by an edge. In this way, a set of mesh nodes contending on the same channel can be modeled as a clique. Previous work in the literature have used the concept of clique applied to wireless networks, such as [33], [34] and [35]. While the concept of clique in those papers is similar to our link group concept, they are several key differences and novelties in our approach. First, [33] targets a different objective. In particular, [33] only provides upper and lower bounds on performance, while our paper aims at providing throughput guarantees while maximizing the number of flows admitted to the network. Second, [33] does not consider heterogeneous transmission rates, i.e., it assumes that all stations use the same modulation scheme (note that in [33], heterogeneous rates refers to different traffic generation rates and not different modulation coding schemes). Furthermore, in [33] traffic differentiation is based on the TXOP parameter, not supported by the standard DCF operation (which is the mechanism we focus on in our paper). Finally, the capacity region in [33] is computed assuming a large number of stations, which is suboptimal in cliques with a small number of stations. In contrast, our computation of the capacity region is more accurate since we take into account the actual number of stations. In [34], authors use the clique concept to reduce the complexity of hand-over operations in wireless mesh networks. More specifically, the network is partitioned in set of routers (i.e., cliques), with one router being elected as the responsible for all mobility operations within each group. Therefore the concept of a clique in [34] is very different from the link group concept in our paper. Finally in [35] the authors consider a TDMA-based wireless multi-hop network and target the minimum-length schedule of a set of links. This is done through a set of coloring algorithms, which result on minimizing the maximum clique around the gateways on the conflict graph, hence reducing the bottleneck schedules around gateway nodes. Therefore, while this concept of a clique is similar to ours, it is used for a very different purpose.

Concerning routing algorithms for wireless mesh networks, the first proposals were based on algorithms already available for mobile ad-hoc networks (e.g.,

shortest path); however, given that mesh networks significantly differ from MANETS [36], these are far from providing optimal performance. Following this observation, some previous works have proposed new metrics for mesh routing [20, 24, 37, 36], tailored to IEEE 802.11 WLANs: ETX [20] is based on the number of attempts to send a frame using lowest-modulation probes; ETT [24] extends it to account for the physical rate and frame length used; ML [37] proposes to find the route with the minimum end-to-end loss probability; while mETX and ENT [36] extend ETX to account not only for average values but also for standard deviations. As opposed to these approaches, our proposal formulates routing as an optimization problem and provides an approximate solution to this problem, which yields a substantially improved performance as we have showed in Section 3. A first attempt to use a linear model to optimize the throughput allocation is the work of [38]. However, the performance of the MAC protocol is not taken into account, and authors assume that the nominal capacity coincides with the achievable capacity of the WLAN. Other works such as [39] aim at modeling routing strategies as solutions of a constrained optimization problem, which is related to our contribution (routing as a multi-commodity flow problem) but their focus is set on wired networks.

Energy optimization is nowadays drawing significant attention from the research community. Although much of the research in this area is focused on optimizing the MAC and the physical layer (e.g., [40]), as well as extending the routing algorithm metric (e.g., in [41] authors propose to use the physical distance), there are some proposals that, like ours, aim at minimizing the energy consumption by means of smart routing, by switching off those nodes not required to support the traffic load. In [42] the authors propose to switch off nodes in areas with high density of routers through a randomized algorithm, therefore leading to non-optimal solutions. In [43] the authors propose, for the case of a mobile operator network, to change users' association in order to switch off as many base stations as possible. However, they propose the use of heuristics which results also in non-optimal performance. A similar approach is presented in [44]; however, this approach focuses on wired networks and is based on heuristics, in contrast to our proposal which takes into account the constraints resulting from wireless links and is formulated as an optimization problem.

6. Conclusions

In this paper we have proposed a novel routing algorithm for wireless mesh networks. The proposed algorithm has been specially devised for mesh networks

owned by operators as i) it relies on carefully planned mesh networks that, by doing proper channel assignment, do not suffer from interference between different link groups, ii) it is based on a centralized algorithm that is executed at a central location and is responsible for the entire routing in the network, and iii) it has been carefully designed to satisfy operator requirements in terms of service guarantees and energy consumption.

The proposed routing algorithm relies on the *linearized capacity region* concept. This is a linear representation of the capacity region of a link that covers almost the entire region, hence allowing almost any of the possible throughput allocations in the link group. Its linearity is a key feature of the proposed concept since relying on linear constraints allows designing efficient optimization algorithms. In this paper, we present an analysis of the capacity region of 802.11 and, based on this analysis, we obtain the corresponding *linearized capacity region*.

One of the key objectives of the proposed routing algorithm is that it provides users with *throughput guarantees*. This is performed by taking into account that the number of flows admitted at a given link group does not exceed the available resources as given by the *linearized capacity region*. In particular, the routing algorithm has been formulated as an *integer programming* problem that admits as many flows as possible while meeting this constraint. This problem is solved by using standard relaxation techniques that provide an approximation to the optimal solution at a reasonably low computational complexity.

Another key objective of the proposed algorithm is that it minimizes the overall energy consumed by the mesh network. Based on existing models on the energy consumption of a node, that show that the energy consumed by an active node is approximately constant independent of its transmission behavior, our routing solution aims at switching off as many nodes as possible. We implement this by adding to our *integer programming* formulation of the routing problem virtual flows and imposing the constraint that routers can either route virtual flows or normal flows, which allows switching off those routers that route virtual flows only.

The approaches proposed in this paper have been extensively evaluated via simulation and compared to previous approaches. The main conclusions drawn from the conducted performance evaluation study are:

i) The proposed linearized capacity region covers most of the actual capacity region of an 802.11 WLAN independent of the modulation rates and the number of flows. This validates the efficiency of the linearized capacity region concept.

ii) The proposed routing strategy outperforms very substantially standard *de facto* strategies such as ETT, ETX and shortest path in terms of throughput. In particular, with the proposed scheme we improve the amount of traffic that can be admitted into the network by a factor that ranges from 2 to 4.

iii) For a given level of traffic in the network, the proposed routing algorithm reduces energy consumption very significantly as compared to previous approaches. In particular, the proposed scheme can provide energy savings of up to 40%.

References

[1] D. Meyer, BT to create wireless cities, Online Article, (2006).

[2] A. Raniwala, K. Gopalan, T. Chiueh, Centralized channel assignment and routing algorithms for multi-channel wireless mesh networks, SIGMOBILE Mobile Computer Communications Review (2004).

[3] P. Serrano, C. Bernardos, A. de la Oliva, A. Banchs, I. Soto, M. Zink, FloorNet: Deployment and Evaluation of a Multihop Wireless 802.11 Testbed, Eurasip, Journal on Wireless Communications and Networking (2009).

[4] P. Serrano, A. de la Oliva, C. Bernardos, I. Soto, A. Banchs, A. Azcorra, A CARMEN Mesh Experience: Deployment and Results, Proceedings of the 1st IEEE WoWMoM Workshop on Hot Topics in Mesh Networking (2009).

[5] J. Restrepo, C. Gruber, C. Machuca, Energy profile aware routing, Communications (ICC) Workshops, IEEE International Conference on (2009).

[6] A. Corliano, M. Hufschmid, Energieverbrauch der mobilen kommunikation, Bundesamt fur Energie, Ittigen, Switzerland, Tech. Rep (2008).

[7] S. Bhaumik, G. Narlikar, S. Chattopadhyay, S. Kanugovi, Breathe to stay cool: adjusting cell sizes to reduce energy consumption, Proceedings of the first ACM SIGCOMM workshop on Green networking (2010).

[8] M. Marsan, L. Chiaraviglio, D. Ciullo, M. Meo, Optimal energy savings in cellular access networks, Proceedings of GreenComm (2009).

[9] G. Bianchi, Performance analysis of the IEEE 802.11 distributed coordination function, IEEE Journal on selected areas in communications (2000).

[10] IEEE Standard for Information Technology-Telecommunications and Information Exchange Between Systems-Local and Metropolitan Area Networks-Specific Requirements - Part 11: Wireless LAN Medium Access Control (MAC) and Physical Layer (PHY) Specifications, IEEE Std P802.11-2007 (2007).

[11] A. Conn, N. Gould, P. Toint, Trust-region methods, Society for Industrial Mathematics, (2000).

[12] M. Bagnulo, Threat Analysis for TCP Extensions for Multipath Operation with Multiple Addresses, RFC 6181, Internet Engineering Task Force, (2011).

[13] A. Ford, C. Raiciu, M. Handley, S. Barre, J. Iyengar, Architectural Guidelines for Multipath TCP Development, RFC 6182, Internet Engineering Task Force, (2011).

[14] GNU Project, GNU Linear Programming Kit. Reference manual for GLPK Version 4.45 (2010).

[15] G. Pataki, M. Tural, E. Wong, Basis reduction and the complexity of branch-and-bound, Proceedings of the Twenty-First Annual ACM-SIAM Symposium on Discrete Algorithms (2010).

[16] Y. Azar, O. Regev, Strongly polynomial algorithms for the unsplittable flow problem, Integer Programming and Combinatorial Optimization, Lecture Notes in Computer Science, Springer (2001).

[17] J. Moy, OSPF Version 2, RFC 2328, Internet Engineering Task Force, (1998).

[18] A. Raniwala, T. Chiueh, Architecture and algorithms for an IEEE 802.11-based multi-channel wireless mesh network, Proceedings IEEE INFOCOM 2005. 24th Annual Joint Conference of the IEEE Computer and Communications Societies (2005).

[19] J. Crichigno, M. Wu, W. Shu, Protocols and architectures for channel assignment in wireless mesh networks, Ad Hoc Networks, Elsevier (2008).

[20] R. Draves, J. Padhye, B. Zill, Routing in multi-radio, multi-hop wireless mesh networks, Proceedings of the 10th annual international conference on Mobile computing and networking (2004).

[21] A. Adya, P. Bahl, J. Padhye, A. Wolman, L. Zhou, A Multi-Radio Unification Protocol for IEEE 802.11 Wireless Networks, Proceedings of the First International Conference on Broadband Networks, IEEE Computer Society (2004).

[22] J. Kim, S. Kim, S. Choi, D. Qiao, CARA: Collision-aware rate adaptation for IEEE 802.11 WLANs, Proceedings IEEE INFOCOM 2006. 25th Annual Joint Conference of the IEEE Computer and Communications Societies (2006).

[23] P. Serrano, A. Banchs, P. Patras, A. Azcorra, Optimal Configuration of 802.11e EDCA for Real-Time and Data Traffic, IEEE Transactions on Vehicular Technology (2010).

[24] D. Couto, D. Aguayo, J. Bicket, R. Morris, A high-throughput path metric for multi-hop wireless routing, Wireless Networks, Springer (2005).

[25] P. Gupta, P. Kumar, The capacity of wireless networks, IEEE Transactions on information theory (2000).

[26] A. Jovicic, P. Viswanath, S. Kulkarni, Upper bounds to transport capacity of wireless networks, IEEE Transactions on Information Theory (2004).

[27] S. Ahmad, A. Jovičić, P. Viswanath, On outer bounds to the capacity region of wireless networks, IEEE/ACM Transactions on Networking (TON) (2006).

[28] A. Zemlianov, G. de Veciana, Capacity of ad hoc wireless networks with infrastructure support, IEEE Journal on selected areas in Communications (2005).

[29] P. Zhou, X. Wang, R. Rao, Asymptotic Capacity of Infrastructure Wireless Mesh Networks, Mobile Computing, IEEE Transactions on (2008).

[30] M. Kodialam, T. Nandagopal, Characterizing the capacity region in multi-radio multi-channel wireless mesh networks, Proceedings of the 11th annual international conference on Mobile computing and networking (2005).

[31] J. Zhang, H. Wu, Q. Zhang, B. Li, Joint routing and scheduling in multi-radio multi-channel multi-hop wireless networks, Broadband Networks (Broad-Nets), 2nd International Conference on (2005).

[32] S. Toumpis, A. Goldsmith, Capacity regions for wireless ad hoc networks, IEEE Transactions on Wireless Communications (2003).

[33] Y. Cheng, H. Li, P. Wan, X. Wang, Capacity region of a wireless mesh backhaul network over the csma/ca mac, Proceedings IEEE INFOCOM 2010. 29th Annual Joint Conference of the IEEE Computer and Communications Societies (2010).

[34] J. Rezgui, A. Hafid, M. Gendreau, B. Rong, Congestion-aware clique-based handoff in wireless mesh networks, Fifth International Conference on Mobile Ad-hoc and Sensor Networks (2009).

[35] C. Gomes, S. Pérennes, H. Rivano, Bottleneck analysis for routing and call scheduling in multi-hop wireless networks, Global Telecommunications Conference. IEEE GLOBECOM Workshops (2008).

[36] C. Koksal, H. Balakrishnan, Quality-aware routing metrics for time-varying wireless mesh networks, IEEE Journal on Selected Areas in Communications (2006).

[37] D. Passos, D. Teixeira, D. Muchaluat-Saade, L. Magalhães, C. Albuquerque, Mesh network performance measurements, International Information and Telecommunicatios Technologies Symposium (I2TS) (2006).

[38] V. Ramamurthi, A. Reaz, B. Mukherjee, Optimal Capacity Allocation in Wireless Mesh Networks, Global Telecommunications Conference. IEEE GLOBECOM (2008).

[39] F. Kuipers, P. Van Mieghem, T. Korkmaz, M. Krunz, An overview of constraint-based path selection algorithms for QoS routing, IEEE Communications Magazine (2002).

[40] C. Jones, K. Sivalingam, P. Agrawal, J. Chen, A survey of energy efficient network protocols for wireless networks, Wireless Networks, Kluvier (2001).

[41] S. Doshi, S. Bhandare, T. Brown, An on-demand minimum energy routing protocol for a wireless ad hoc network, ACM SIGMOBILE Mobile Computing and Communications Review (2002).

[42] B. Chen, K. Jamieson, H. Balakrishnan, R. Morris, Span: An energy-efficient coordination algorithm for topology maintenance in ad hoc wireless networks, Wireless Networks, Springer (2002).

[43] K. Dufková, M. Bjelica, B. Moon, L. Kencl, J. L. Boudec, Energy savings for cellular network with evaluation of impact on data traffic performance, European Wireless 2010 (2010).

[44] L. Chiaraviglio, M. Mellia, F. Neri, Energy-aware networks: Reducing power consumption by switching off network elements, FEDERICA-Phosphorus tutorial and workshop (TNC2008) (2008).